35th Annual International Conference of the IEEE EMBS
Osaka, Japan, 3 - 7 July, 2013

A biomimetic framework for coordinating and controlling whole body movements in humanoid robots

Pietro Morasso, Francesco Rea, and Vishwanathan Mohan

Abstract— **An integrated model for the coordination of whole body movements of a humanoid robot with a compliant ankle similar to the human case is described. It includes a synergy formation part, which takes into account the motor redundancy of the body model, and an intermittent controller, which stabilizes in a robust way postural sway movements, thus combining the hip strategy with ankle strategy.**

I. INTRODUCTION

A biomimetic approach for synergy formation of whole body movements in humanoid robots is described in [1]. It is based on PMP (Passive Motion Paradigm) which uses abstract force fields for representing task goals and internal/external constraints. This formalism has been used for simulating whole body reaching movements of the iCub robot [2] during upright standing [3], thus combining a double task: 1) a *focal task* (reaching or approaching as much as possible a target in 3D space) and 2) a *postural task* (keeping the vertical projection of the center of mass (CoM) inside the support base of the standing body). In particular, this synergy formation mechanism uses two external force fields (one applied to the hands for the focal part and the other applied to the pelvis for the postural part, thus implementing a *hip strategy* of stabilization) and several internal fields for enforcing joint limits. The simulated patterns generated by the model [3] are consistent with distinctive aspects of human behavior for this kind of task, namely the synchronized velocity peaks of the reaching hand and the forward shift of the center of mass (CoM). However, this PMP-based mechanism is *mass-less* and is not yet a control system because it does not provide specific stabilization signals of the inverted pendulum which, at least approximately, represents the standing body. The intrinsic instability of the inverted pendulum model is due to the fact that the rate of growth of the gravity-related toppling torque is greater than the stiffness of the critical joint involved in the stabilization of the standing body, namely the ankle. Therefore, a controller is needed for providing ankle torque control signals that stabilize the inverted pendulum. In a previous paper [4] an intermittent controller was described which achieves bounded stability in a robust way by means of a simple PD (proportional + derivative) control action, which is switched on/off by a decision mechanism based on the analysis of the trajectories of the inverted pendulum in the phase space.

*Supported by EU DARWIN project, Grant No: FP7-270138 and by US Army NSRDEC, Grant No. W911QY-12-C-0078.

The authors are with the Istituto Italiano di Tecnologia, RBCS dept., 16063 Genoa, Italy (phone: +39 0103991798; fax: +39 0103991798).
Pietro Morasso: pietro.morasso@ iit.it.
Francesco Rea: francesco.rea@ iit.it.
Vishawanathan.Mohan: vishwanathan.mohan@ iit.it.

This paper is a preliminary study on the feasibility of extending the intermittent controller from quiet standing to dynamic standing, as in whole body reaching movements. It integrates the PMP synergy formation mechanism, which generates time-varying reference postures of the body, including the tilt angle $\theta_{ref}(t)$ of the CoM, with the intermittent controller which switches on/off the feedback control law according to the current state of the pendulum [θ, $d\theta/dt$].

II. THE INTEGRATED MODEL

Fig. 1 shows a simplified block diagram of the combined model: the top part corresponds to the PMP network and the bottom part to the intermittent controller. The two parts interact in a bidirectional manner, thus integrating the *hip strategy*, implemented by the PMP network, with the *ankle strategy*, implemented by the intermittent controller.

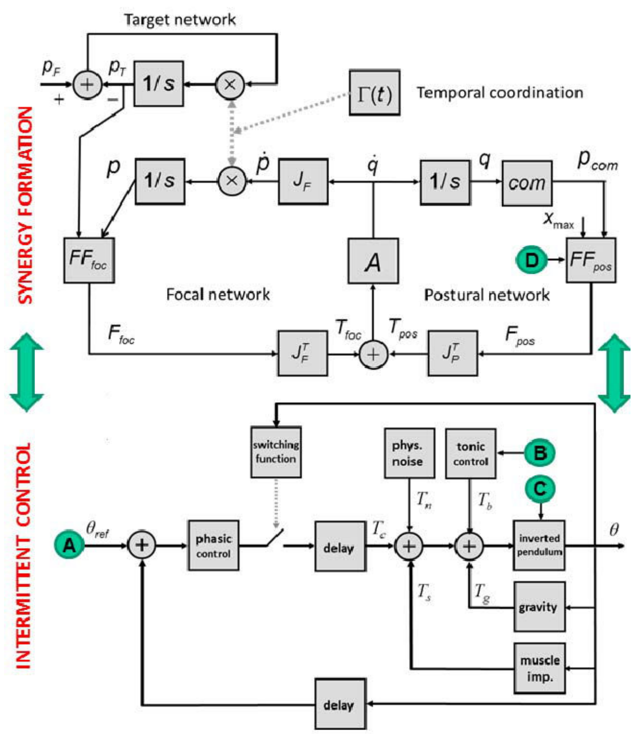

Figure 1. Block diagram of the overall control system.

The green labeled circles correspond to the interaction ports among the two parts, as better explained in the following.

A. The synergy formation part (PMP network)

The PMP network includes three sub-networks: 1) a target sub-network, which generates a moving target from the initial position of the end-effector to the final intended target; 2) a focal sub-network, which attracts the end-effector to the moving target according to a *Focal Force Field*; 3) a postural sub-network, which pulls back the pelvis according to a *Postural Force Field,* as a function of the distance of the CoM from the allowed limit of stability:

$$\begin{cases} p_F = [x_F, y_F, z_F]: \text{ final target position} \\ p_T = [x_T, y_T, z_T]: \text{ moving target position} \\ p = [x, y, z]: \text{ (virtual) trajectory of the end-effector} \end{cases}$$

For simplicity, but without any loss of generality, we limit the analysis to the sagittal plane [*x, z*]: x_{com} represents the forward/backward shift of the CoM and x_{max} the maximum forward position allowed by the size of the support base. The two force fields are computed as follows:

$$\begin{cases} F_{foc} = K_F\left(p_T - p\right) \\ F_{pos} = -K_P \begin{bmatrix} \dfrac{x_{com}}{x_{\max} - x_{com}} \\ 0 \end{bmatrix} \end{cases} \tag{1}$$

The network includes two *Jacobian matrices*: J_F for the focal sub-network (it is a 2×6 matrix, related to 6 joints of the body model: ankle, knee, hip, shoulder, elbow, wrist) and J_P for the postural sub-network (it is a 2×3 matrix, related to 3 joints: ankle, knee, hip). *A* is an *admittance matrix* (6×6 diagonal) which encodes the relative degree of participation of the different joints to the global movement. Γ(t) is the temporal coordination module that allows the synchronization of the two tasks, determining terminal attractor properties for the overall network [1].

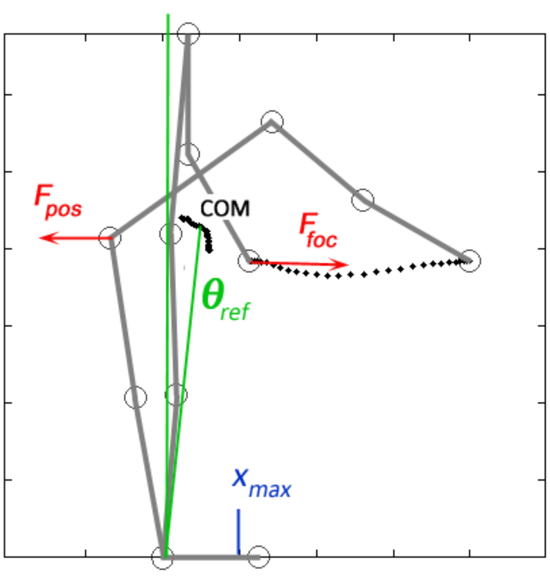

Figure 2. Virtual force fields that operate on the body schema.

Fig. 2 illustrates how the virtual force fields operate on the body schema. The trajectory of the end-effector is synchronized with the trajectory of the CoM, which is shifted forward and downward, without overcoming the stability margin x_{max}.. This determines also an evolution over time of the tilt angle of the CoM: $\theta_{ref}(t)$. Movement patterns are generated as transients from an equilibrium state to another equilibrium state, solving implicitly the redundancy of the robot body schema without any explicit optimization.

B. The intermittent control part

In this preliminary study, the dynamics of the overall body is reduced to the dynamics of the equivalent inverted pendulum. An important point is that the length of the pendulum is not constant, as in the analysis of quiet upright standing, but changes over time, thus determining a time-varying moment of inertia of the pendulum. Thus, in the bottom panel of fig. 1 the “inverted pendulum” block is characterized by the following transfer function, where T_{tot} is the total torque applied to the ankle:

$$\frac{\theta(s)}{T_{tot}(s)} = \frac{1}{I s^2} \tag{2}$$

The moment of inertia *I* is a function of the body posture (I=$I(q)$) thus connecting the synergy formation part of the model with the control part. Other elements of dynamic interaction between the two parts are the tonic and phasic parts of the controller.

T_{tot} comprises five components, namely gravity (T_g); muscle stiffness (T_s); noise (T_n); tonic control (T_b); phasic control (T_c):

$$\begin{cases} T_g = Mgh \cdot \theta \\ T_s = -K_m \cdot \theta - B_m \cdot \dot{\theta} \end{cases} \tag{3}$$

For the intrinsic ankle impedance we assumed that stiffness K_m is 70% of the destabilizing coefficient *Mgh* in the upright standing position and the damping coefficient B_m is 4 Nm/rad/s. The noise term is a filtered white noise (cutoff frequency 4 Hz) with a RMS value of 0.2 Nm.

The tonic part of the control compensates for the static toppling torque due to gravity, for the reference angle θ_{ref} generated by the PMP model:

$$T_b = -Mgh \cdot \theta_{ref} \tag{4}$$

The phasic part of the control, aimed at dynamic bounded stabilization, is computed by the intermittent controller [4], which activates the PD control torque T_c in an intermittent manner, according to the following activation rule, illustrated by graph in figure 3:

$$\begin{cases} \Delta\theta_\delta = \theta_{ref}(t-\delta) - \theta(t-\delta) \\ \text{if } \ \Delta\theta_\delta\left(\Delta\dot{\theta}_\delta - a\,\Delta\theta_\delta\right) > 0 \\ \quad \text{then} \qquad T_c = K_1 \Delta\theta_\delta + K_2\, d\Delta\theta_\delta / dt \\ \quad \text{otherewise} \ \ T_c = 0 \end{cases} \tag{5}$$

δ is the delay of efferent & afferent signals and was set equal to 0.2s; *a* is the slant of the decision line in the phase plane of the inverted pendulum and was set to $-0.4s^{-1}$; K_1=27.55N/m is the proportional gain of the PD controller (it must satisfy a necessary condition for static stability: $K_1 > Mgh - K_m$); K_2=10Nms/rad is the corresponding derivative gain.

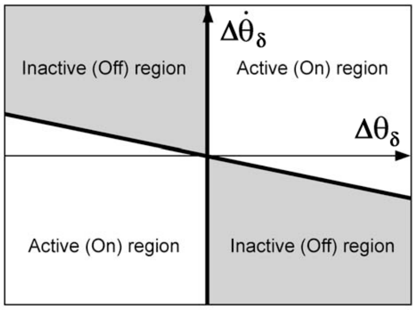

Figure 3. Activation rule of the Intermittent Controller, in the phase plane of the inverted pendulum.

Considering that the instability of the inverted pendulum is of saddle-type, which includes an unstable manifold (a line in the first/third quadrant of the phase plane) but also a stable manifold (a line in the second/fourth quadrant), the switching rule above can be rephrased as follows: active control is engaged when the motion of the pendulum occurs in the neighborhood of the unstable manifold but the pendulum is allowed to evolve freely when it operates near the stable manifold. The remarkable fact, as shown in [4], is that even if the two regimes (forced and unforced) are globally unstable, the combined intermittent controller can achieve bounded stability, despite the delay of feedback signals, as we show in the following section.

C. The ports of interaction between the two networks

As shown in figure 1, there are four ports (labeled **A**, **B**, **C**, **D**, respectively) where the two networks interact, inducing an overall integrated dynamics:

A: The reference angle for the intermittent controller $\theta_{ref}(t)$ is the angle of the line that links the center of mass of the body schema to the ankle. It is a function of the vector of joint angles q and the distribution of masses in the body. It is computed by a block included in the PMP network;

B: The tonic torque component of the ankle controller also requires $\theta_{ref}(t)$ and uses eq. 4;

C: The inverted pendulum model takes into account the actual length of the pendulum, as computed by the PMP network;

D: The postural force field, in the integrated model, takes into account the position of the CoM in the sagittal plane, in relation with the maximum allowed forward displacement x_{max}, as computed by both networks: the PMP network computes x_{com} as a function of θ_{ref} and the intermittent controller computes x_{com} as a function of θ. The overall postural field is a weighted combination of the two fields:

$$F_{pos} = -K_{P1}\frac{x_{com}(\theta_{ref})}{x_{\max} - x_{com}(\theta_{ref})} - K_{P2}\frac{x_{com}(\theta)}{x_{\max} - x_{com}(\theta)} \qquad (6).$$

In this preliminary study, the dynamics of the overall system is simulated by means of Matlab©, Simulink©, and SimMechanics© (MathWorks, Inc., Natick Mass. USA).

III. Results

Figure 4 shows a simulation of the integrated model, with the robometric parameters of the iCub robot (see also table I). Note that in this simulation the target is outside the reachable workspace, nonetheless the controller finds the final posture that approaches the target as much as possible (see the red trajectory of the end-effector and the stretched out final posture of trunk and arm). The movement of the end-effector is accompanied by the movement of the CoM (green trajectory in figure 4).

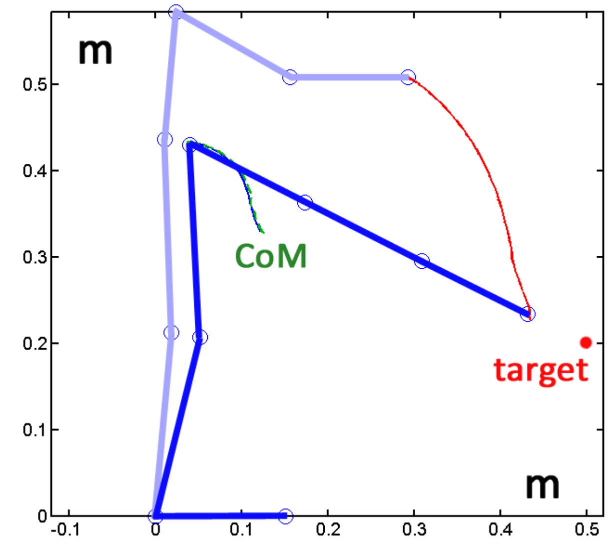

Figure 4. Initial and final posture of the stick figure of the body.

Figure 5 shows an expanded view, plotting both the CoM trajectory generated by the PMP network alone (blue line) and the trajectory resulting from the combined intermittent controller (green dashed line). The red dotted line corresponds to x_{max} and the figure shows that the integrated model succeeds to keep the CoM in the safe area while attempting to reach the target.

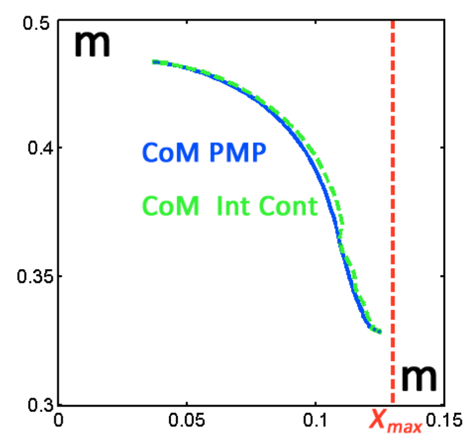

Figure 5. Trajectories in the sagittal plane of the CoM generated by the PMP and the Intermittent controller, respectively.

The trajectories of the end-effector and the CoM are roughly synchronized, as shown in figure 6: the green line represents the distance between the end-effector and the target; the blue line is the sagittal component of the CoM shift. Again, note that the CoM stops short of the critical limit x_{max}.

The interplay between the two postural components of the overall control system is also represented in figure 7, which shows the evolution of the state vector in the phase plane of the inverted pendulum.

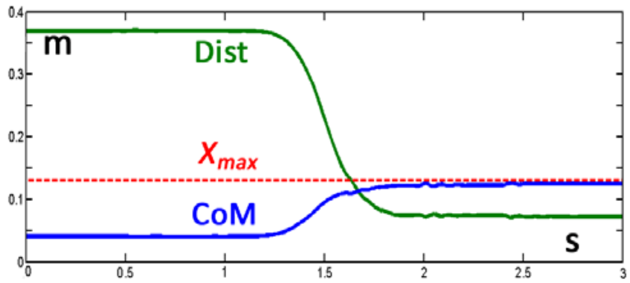

Figure 6. Time course of the CoM and the distance (Dist) of the end-effector from the target.

At the beginning of the simulation, the body is standing up and the CoM is slightly tilted forward (about 0.08rad = 4.5 deg). The sway movements in this situation have a rather small amplitude and are determined by the interplay between the intermittent controller and the noise source. When the final target is instantiated, a time-varying reference angle of the equivalent inverted pendulum is generated by the PMP network, which shifts the unstable equilibrium in the phase plane to a greater angle (0.36rad), but smaller than the critical value associated with the x_{max} parameter. After the transient, the state vector stabilizes around the new tilt angle with sway movements of larger amplitude, but still compatible with an overall bounded stability of the body.

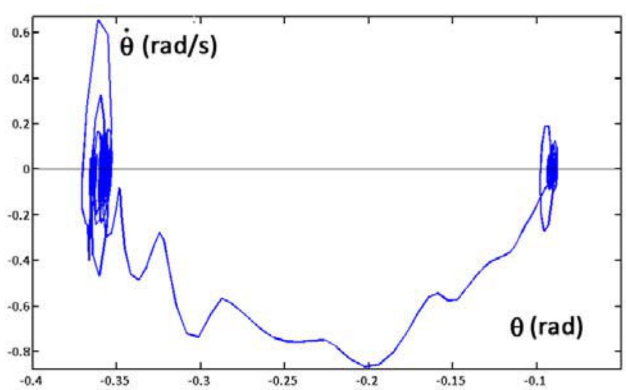

Figure 7. Evolution of the state vector in the phase plane of the inverted pendulum from the initial posture (sway pattern in the right part of the graph) to the final posture (sway pattern in the left part of the graph).

The increased sway size can be attributed to the fact that the parameters of the intermittent controller, selected specifically in order to match the initial posture, are kept constant throughout the overall simulation and thus operate in a less favorable region. The capability of the integrated system to recover equilibrium in the new final posture, after the whole body movement, is strongly related on the feedback from the intermittent controller to the PMP network via the postural force field. Without the second element of eq. 6, which takes into account the actual tilt angle of the inverted pendulum to be combined with the reference tilt angle, the return to stability could be disrupted.

IV. Discussion

The first conclusion that we may draw from the simulation results is that the robustness of the intermittent controller, previously evaluated in quiet standing [4] is preserved also in whole body movements. The model captures the nature of so called Anticipatory Postural Adjustments [5]: the PMP network embodies the anticipatory part of the mechanism, which operates according to a hip strategy; the intermittent controller compensates the intrinsic instability due to the compliant ankle.

Different extensions of the model can be envisaged. One is to substitute the intermittent controller, operating on a single inverted pendulum, with a controller operating on a multi-link inverted pendulum, taking into account the results found by Suzuki et al [6].

Another one is to investigate the effect of loading the body model and the appropriate modifications of the stabilization mechanisms.

TABLE I.

Model parameters	
Parameter	***Values***
Link lengths (foot, shin, thigh, trunk, humerus, forearm+hand) [m]	0.15; 0.213; 0.224; 0.149; 0.152; 0.1370.
Link weights (shin, thigh, trunk, humerus, forearm+hand) [kg]	0.95; 1.5; 4; 1.15; 0.5.
Postural cliff x_{max} [m]	0.13 m
Muscle parameters K_m, B_m [Nm/rad, Nms/rad]	27.65; 4.
Slope of decision boundary a [1/s]	0.4.
Afferent/efferent delay δ [ms]	200.
Parameters of PD controller K_1, K_2 [Nm/rad, Nms/rad]	27.55; 10.
Gain of the focal field K_F [N]	700.
Gains of the postural fields K_{P1},K_{P2} [N, N]	4; 4.

References

[1] V. Mohan, P. Morasso, G. Metta, and G. Sandini, "A biomimetic, force-field based computational model for motion planning and bimanual coordination in humanoid robots," *Autonomous Robots*, vol. 27, pp. 291-307, 2009.

[2] www.icub.org

[3] P. Morasso, M. Casadio, V. Mohan, and J. Zenzeri, "A neural mechanism of synergy formation for whole body reaching," *Biol. Cybern.*, vol. 102, pp. 45-55, 2010.

[4] Y. Asai, Y. Tasaka, K. Nomura, T. Nomura, M. Casadio, and P. Morasso, "A model of postural control in quiet standing: robust compensation of delay-Induced Instability using intermittent activation of feedback control," *PLoS One*, vol. 4(7):e6169, 2009.

[5] S. Bouisset and M. Zattara, "Biomechanical study of the programming of anticipatory postural adjustments associated with voluntary movement", *J. Biomech*., vol. 20, pp. 735–742, 1987.

[6] Y. Suzuki, T. Nomura, M. Casadio, and P. Morasso, "Intermittent control with ankle, hip, and mixed strategies during quiet standing: A theoretical proposal based on a double inverted pendulum model, " *J. Theoretical Biology*, vol. 301, pp. 55-79, 2012.